AO4ELT7 - June 2023 - Avignon

Optimizing atmospheric turbulence predictions for optical links and astronomical observations

M.J. Medlej, C. Giordano, A. Ziad, S. Prunet, A. Rafalimanana, and E. Aristidi

Université Côte d'Azur, Observatoire de la Côte d'Azur, CNRS, Laboratoire Lagrange, France

ABSTRACT

The prediction of the atmospheric and turbulence conditions are of great interest for the astronomical community and free space optical telecommunications. With the advent of the next generation of extremely large telescopes (ELT), the knowledge of atmospheric conditions several hours prior to observations has become essential. As well, in the field of free space optical telecommunications, the propagation of optical signals in the atmosphere is significantly influenced by weather conditions (clouds, fog, rain, etc.) and optical turbulence. A numerical approach based on the Weather and Research Forecasting (WRF) model coupled with an optical turbulence model for the predictions above the Calern site has been used. Results have shown good agreement between predictions and observation. However, a difference persists in the first 500 m of the atmosphere. We present in this paper two approaches to improve the predictions. The first one has been developed by Giordano et al.[1] using a 'site learning' method. The second one consists of using data from an instrumented drone to improve the initial conditions of the simulations. We will also present a new method for short-term prediction using two statistical learning algorithms: ARIMA (Autoregressive Integrated Moving Average) and SARIMA (Seasonal Autoregressive Integrated Moving Average).

1. INTRODUCTION

Turbulence is a natural and ubiquitous phenomenon present in various aspects of our universe, influencing both astronomical and telecommunications communities. In astronomy, turbulence affects the quality of observations, limiting our ability to explore the space with very high precision. Therefore, besides the importance of reducing the lost in cost of observations due to bad atmospheric conditions, it is important to specify a site that provides an optimal optical quality. Generally, the objective is to minimize the impact of turbulence on the optical beam as it travels through the atmosphere. Adaptive Optics (AO) techniques are employed to achieve this goal, aiming to mitigate turbulence effects. However, relying solely on AO methods cannot completely eliminate the challenges posed by turbulence. Therefore, there is a critical necessity to develop a robust and efficient tool capable of forecasting atmospheric turbulence conditions several hours in advance. This advancement would facilitate the optimization of astronomical observation plans, following the concept of "Flexible Scheduling".
Similarly, in telecommunication, turbulence introduces complexities in signal propagation, resulting in fading, distortion, and signal losses. These disturbances can significantly impede communication, particularly within free-space optical networks. As a result, it becomes crucial to anticipate the optical ground station that experiences the least turbulence, thus enabling the identification of optimal time frames for laser links, both in transmission

and reception. This approach can be described as "Smart Scheduling." Within this context, the significance of turbulence prediction in both astronomy and telecommunications cannot be emphasized enough.
Previously, our team has developed a numerical approach based on the Weather and Research Forecasting (WRF) model coupled with different optical turbulence models. The results were then compared with in-situ and optical measurements from the Calern Atmospheric Turbulence Station (CATS) (Rafalimanana et al.[4]). In order to improve the predictions, an optimization process by incorporating local measurements to better capture site-specific characteristics was tested by Giordano et al.[1]. This technique, known as "site learning," yielded good results when tested at the Calern Observatory site in France, resulting in better prediction accuracy. Although there has been an improvement in the prediction, some dispersion still persists within the first 500 meters of the atmosphere. In order to improve the predictions in this part of the atmosphere, we have employed an instrumented drone to conduct in-situ measurements of meteorological parameters, including pressure, temperature, humidity, and wind, within the first 500 meters above the ground. The obtained data will contribute to the improvement of the simulations, which will improve the turbulence prediction. On the other hand, we used two statistical learning algorithms, ARIMA and SARIMA, to predict surface weather parameters. This approach can subsequently help us predict the OT vertical profile parameters once we have successfully predicted the vertical weather parameter profile using data from the drone.
This paper is organized as follows. In section 2, we give an overview of the WRF model configuration. Section 3 describes the model of optical turbulence (OT). In Section 4, we will explore the ways to optimize the predictions. Section 5 will present the results stemming from improvements in model validation achieved through the site learning method, the instrumented drone and the statistical learning models. And finally, in section 6 we draw the primary conclusion from our study.

2. WRF SIMULATIONS SETUP

In our research, we used the Weather Research and Forecasting (WRF) model, which was developed by the National Center for Atmospheric Research (NCAR). This model allows us to predict weather parameters which are central for deriving turbulence predictions as illustrated in the Figure 1.
Running a Weather Research and Forecasting (WRF) simulation involves several steps to accurately model atmospheric conditions and predict weather patterns. First one needs to gather the necessary input data, including meteorological observations and terrain information. Next, configure the WRF model by selecting appropriate physics schemes, grid resolutions, and simulation domain. Then, preprocess the data to create initial and boundary conditions for the simulation.

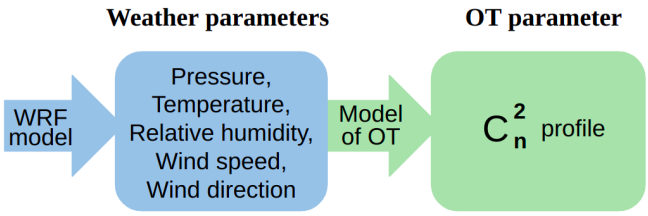

Figure 1: The flowchart for the turbulence prediction.

For our simulations, we used the meteorological input data from the Global Forecast System (GFS) with a resolution of 0.25x0.25 degrees (approximately 111x111 km). To account for the terrain roughness accurately, the topographic data were sourced from the Shuttle Radar Topography Mission (SRTM), providing a resolution of 0.09x0.09 km. The model was configured with four domains of horizontal resolutions varying from 27 × 27 km to 1 × 1 km (Figure 2). Table 1 summarized the configuration of our domains.

Domains	Resolution (km²)	Grid points number	Vertical level number	Vertical resolution (m)
D01	27 x 27	140 x 140	45	Δh_{min} = 23 Δh_{max} = 532
D02	9 x 9	130 x 130	45	
D03	3 x 3	118 x 118	45	
D04	1 x 1	106 x 106	45	

Table 1: The flowchart for the turbulence prediction.

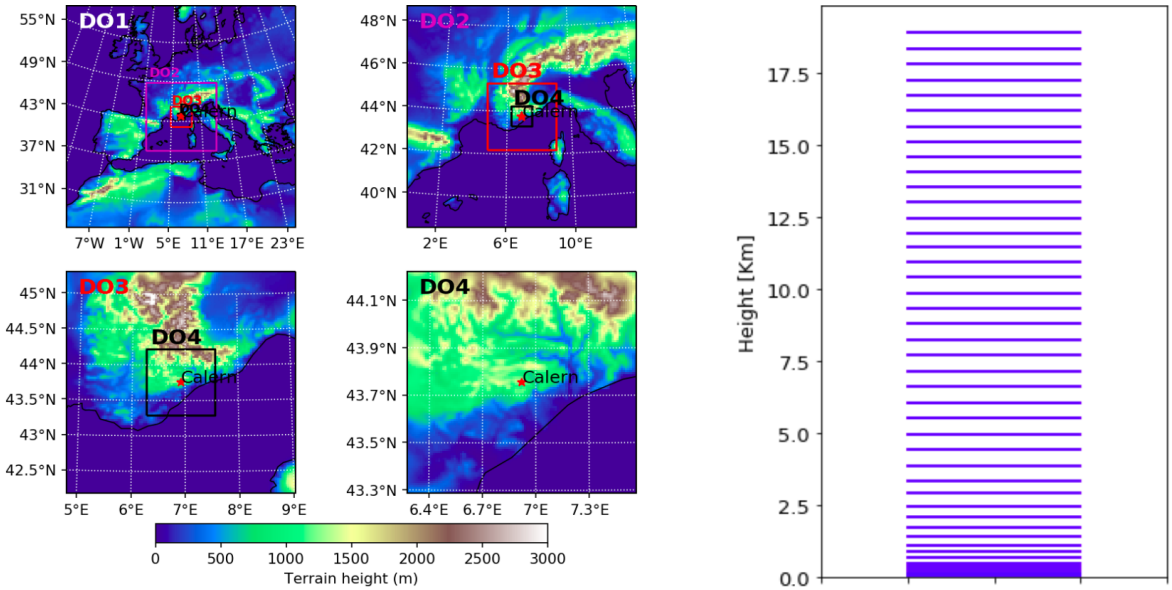

Figure 2: **Left:** topography of the main and nested domains. **Right:** vertical levels of the model.

3. OPTICAL TURBULENCE MODEL

In this study, we used the empirical model developed by Trinquet and Vernin[5]. This model is based on the analysis of data from a large number of radiosondes launched worldwide. The data sets consisted of simultaneous measurements of meteorological parameters (Pressure, Temperature, Relative Humidity, and Wind Velocity) and of the refractive index structure parameter C_n^2. Trinquet and Vernin derived a statistical relationship from these radiosonde measurements, linking the C_n^2 profile to the vertical gradient of horizontal wind shear $S(z)$ and the vertical gradient of mean potential temperature χ(z) given by the equation 1.

$$C_T^2(z) = \phi(z).\chi(z).S(z)^{1/2} \tag{1}$$

In this equation, z represents the altitude and ϕ(z) is a function derived from the data, which represents the statistical profile of the radiosonde balloons given by equation 2.

$$\phi(z) = \frac{\langle C_T^2(z)\rangle_m}{\langle \chi(z)\rangle_m \langle S(z)\rangle_m^{1/2}} \tag{2}$$

where $\langle\rangle_m$ is the median value. The formulas for χ(z) and $S(z)$ are given by the equations 3 and 4.

$$\chi(z) = \frac{d\theta}{dz} \tag{3}$$

$$S(z) = \left[\left(\frac{dV_x}{dz}\right)^2 + \left(\frac{dV_y}{dz}\right)^2\right]^{1/2} \tag{4}$$

where V_x and V_y represent the horizontal components of wind velocity, and θ represents the potential temperature[1]. To derive the C_n^2, we use the Gladstone's law given by equation 5.

$$C_n^2(z) = \left(\frac{80.10^{-6}P(z)}{T(z)^2}\right)^2 .C_T^2(z) \tag{5}$$

where $P(z)$ is the vertical profile of atmospheric pressure in hPa, $T(z)$ is the vertical profile of air temperature in Kelvin.

4. PREDICTION OPTIMIZATION

4.1 Site learning

Giordano et al.[1] implemented a method to enhance the empirical model obtained from balloon radio-soundings. This method consists in incorporating site-specific local statistics to consider the unique characteristics of the site. This method was called site learning (SL). As described in the equation 1, ϕ(z) is the statistical profile depending on available measurements. Giordano et al.[1][2], used sample from the CATS database that corresponds to the same WRF forecasting sample to evaluate the influence of integrating local measurements into the empirical model as a constraint. The results have shown a significant enhancement in comparison to the original empirical method for our forecasting tool. However, there is still some dispersion in predictions primarily attributable to the difficulties of accurately forecast ground conditions due to the complexity of the terrain. To address these issues, we intend to explore the utilization of instrumented drones within the first 500 meters above the ground (section 4.2).

4.2 Instrumented drone

Our experiment consists of an unmanned aircraft system (UAS) equipped with a nacelle containing instruments to measure the meteorological parameters (pressure, temperature, humidity, wind) in the first 500 m above ground. These in-situ measurements of vertical profiles will enable us to improve the turbulence model.
The UAS employed for this study was the DJI Matrice 600 Pro, as illustrated in Figure 3. This UAS model is capable of accommodating a payload of up to 6 kg at maximum capacity, with a flight duration varying from 16 to 38 minutes depending on the transported weight. The nacelle is attached to the drone by a rope 15 to 30m long, and contains different weather stations. Rafalimanana et al.[3] has made several test campaigns on the site of Calern to determine the best configurations for the position of the stations below the drone. Furthermore, he proved that the chosen weather stations were in good agreement with the reference weather stations in Calern.

Figure 3: The instrumented drone.

[1]The potential temperature is the temperature assigned to a parcel of dry air, which represents the temperature that the parcel would have if it were brought adiabatically to a reference pressure level of 1000mb.

To achieve measurements of vertical profiles of meteorological parameters within the first 500m layer of atmosphere, the entire instrument would move vertically above a fixed location, ascending and descending at a rate of approximately 1 meter per second, in order to gather a substantial amount of data with a high vertical precision.
The next step is to inject these data into the WRF model. This is the role of the module "Objective Analysis" (OBSGRID). In our case, pressure, temperature, relative humidity, wind speed, and wind direction profiles from the instrumented drone are used as input into WRF.

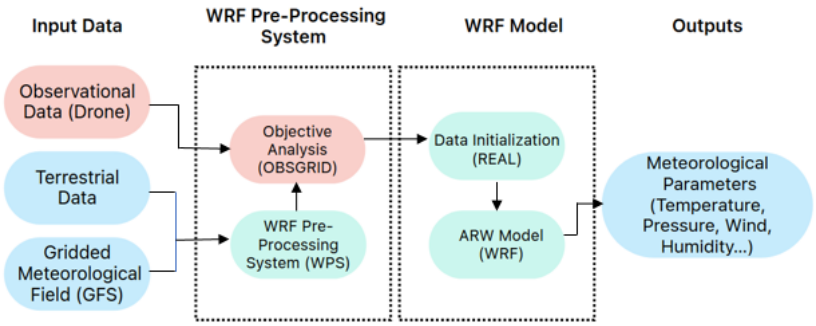

Figure 4: Drone data injection in WRF workflow diagram.

4.3 Statistical learning models

ARIMA and SARIMA models are time series forecasting techniques used to predict data with a temporal component. ARIMA model is typically denoted by ARIMA(p,q,d), where p, d and q represents the three key components of the model. SARIMA model includes additional parameters to model the seasonal component of the data, it's represented by SARIMA(p, d, q)(P, D, Q)s. In both models, the p component represent the relationship between the current value and its past values. The d component, accounts for differencing the data to make it stationary. The q component models the relationship between the current value and past error terms. The next three components (P, D, Q) used in addition for the SARIMA model, are similar to (p, d, q) but pertain to the seasonal part of the model. The 's' is the length of the seasonal cycle. We choose 's' to be equal to 24 as our data is sampled every hour. Concerning the other components, we used pmdarima library in pthon to perform automatic ARIMA and SARIMA components selection.

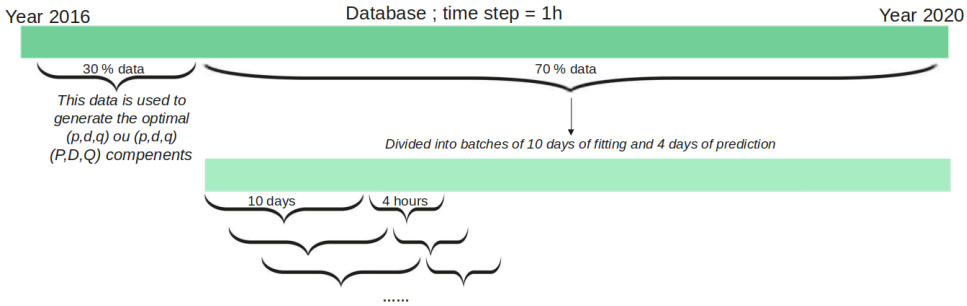

Figure 5: Workflow of the data division for the models.

The data used for this study is the weather surface parameters from the CATS database. As shown in the Figure 5, we used 30% of our data to find the optimal (p,d,q) or (p,d,q)(P,D,Q) components for our model for each weather parameter. The remaining 70% were divided into batches of 10 days of fitting using the optimal (p,d,q) or (p,d,q)(P,D,Q)s and 4 hours of prediction for each weather parameter. The preliminary results are

presented for 500 prediction of 4 hours each. The predictions were compared to measurement by CATS. The preliminary results are encouraging.

5. RESULTS AND DISCUSSION

5.1 Site-learning

In this subsection, we present the impacts of the SL (presented in section 4.1) on the improvement of the turbulence model. Figure 6, shows the median profiles for the entire month of March 2021 of the C_n^2 measured by the PML (Profiler of Moon Limb) provided by the Calern Atmospheric Turbulence at Calern Observatory (Ziad, A. et al.[6]) and predicted by WRF. The associated colored surfaces represent, for each layer, the range between the first and third quartiles. When using the statistical model (radio sounding balloons model) of the optical turbulence (OT) model without SL, a significant disparity is observed between the prediction and the measurement mostly in the lower part of the atmosphere. However, when applying the SL method, the gap is reduced. These results are consistent with those presented in Giordano et al.[1].

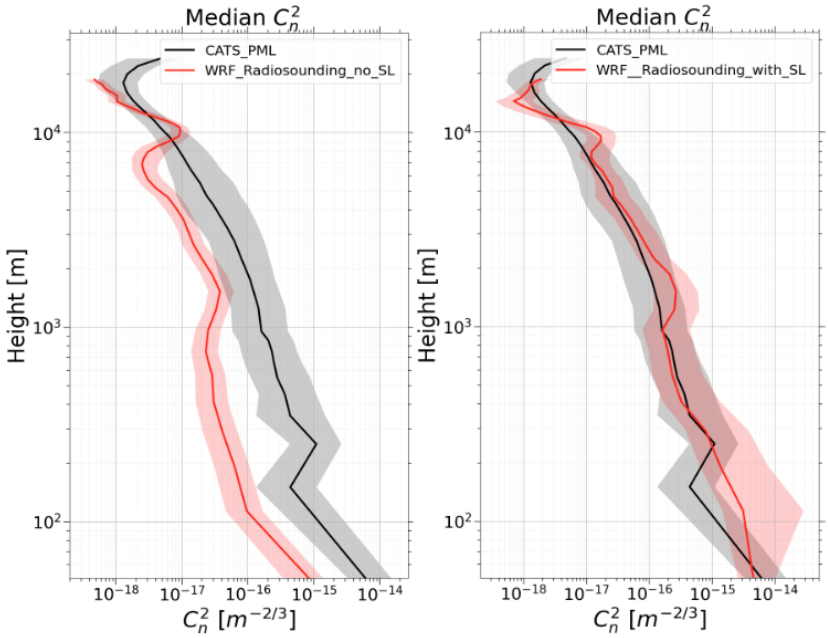

Figure 6: Median vertical profiles of the C_n^2 for the month of March 2021. The black profiles represent measurements by PML. The red profiles are predicted by WRF using the empirical model, with the left side representing predictions made without considering the SL method and the right side showing predictions made with consideration of the SL method. The colored regions show the interval between the first and the third quartiles at each altitude.

Regarding these median profiles, it is observed that WRF without SL underestimates C_n^2 more than WRF with SL when compared to PML measurements. So, this SL method brings a significant improvement to the forecasts. However, it is important to highlight that the prediction of the C_n^2 in the surface layer exhibit significant inaccuracies even after using the SL method. This could be attributed to the difficulties of predicting the ground factors due to the theoretically demanded high resolution.

5.2 Instrumented drone

In the following, we will present the preliminary results of weather parameter prediction using drone data. Simulations with and without using drone data are compared to drone profiles to check the accuray of the

predictions. Figures 7 and 8 presents two instantaneous profiles of weather parameters for two different days. For these two days, we observe that injecting drone observation data into the WRF model using OBSGRID leads to improve the predictions on the temperature.

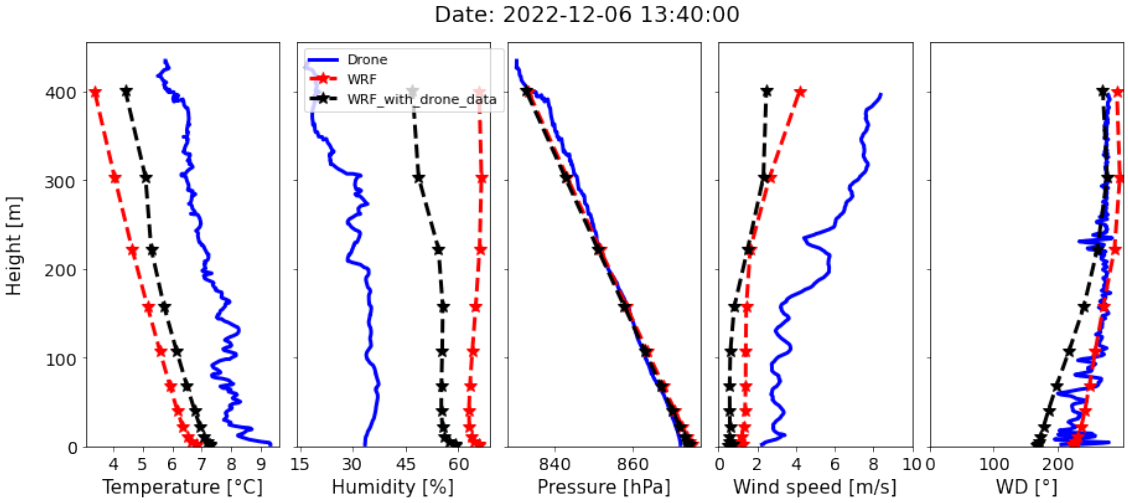

Figure 7: Example of vertical profiles for weather parameters for 12 December 2022. Drone profiles are represented in blue, WRF simulations without drone data in red and WRF simulations with drone data in black.

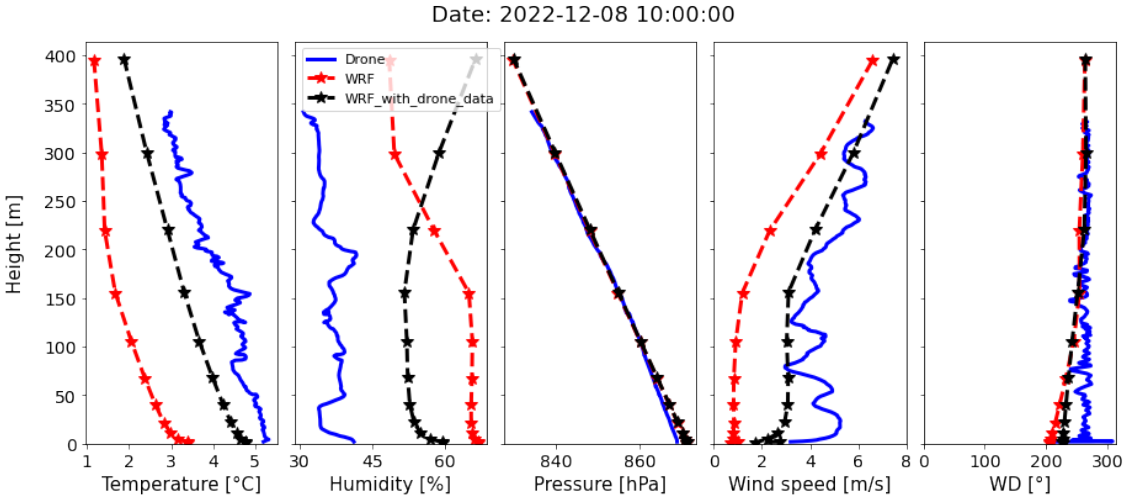

Figure 8: Examples of vertical profiles for weather parameters for 8 December 2022. Drone profiles are represented in blue, WRF simulations without drone data in red and WRF simulations with drone data in black.

Regarding relative humidity, the use of drone data in the simulations improves the prediction for Figure 7, while for Figure 8, improvement is observed up to 250 meters. For wind speed, a significant improvement is seen in Figure 8.

As for wind direction, a slight improvement is observed for Figure 8, however for Figure 7, improvement is observed above 250 meters. For wind speed, a clear improvement is observed in Figure 8.

In general, the improvement in weather parameter prediction will translate into an amelioration in the prediction of OT parameters. However, to draw a definitive conclusion, it is necessary to make more measurements using the drone for a comparative statistical study.

5.3 Statistical learning models

In the following subsection, we will present the preliminary results of forecasting using the SARIMA model for different surface weather parameters. We have chosen to show the SARIMA results due to their superior performance compared to the ARIMA model, primarily attributed to its ability to capture and account for seasonal patterns. However, it's essential to note that the SARIMA model does demand more computational resources and processing time compared to the ARIMA model.

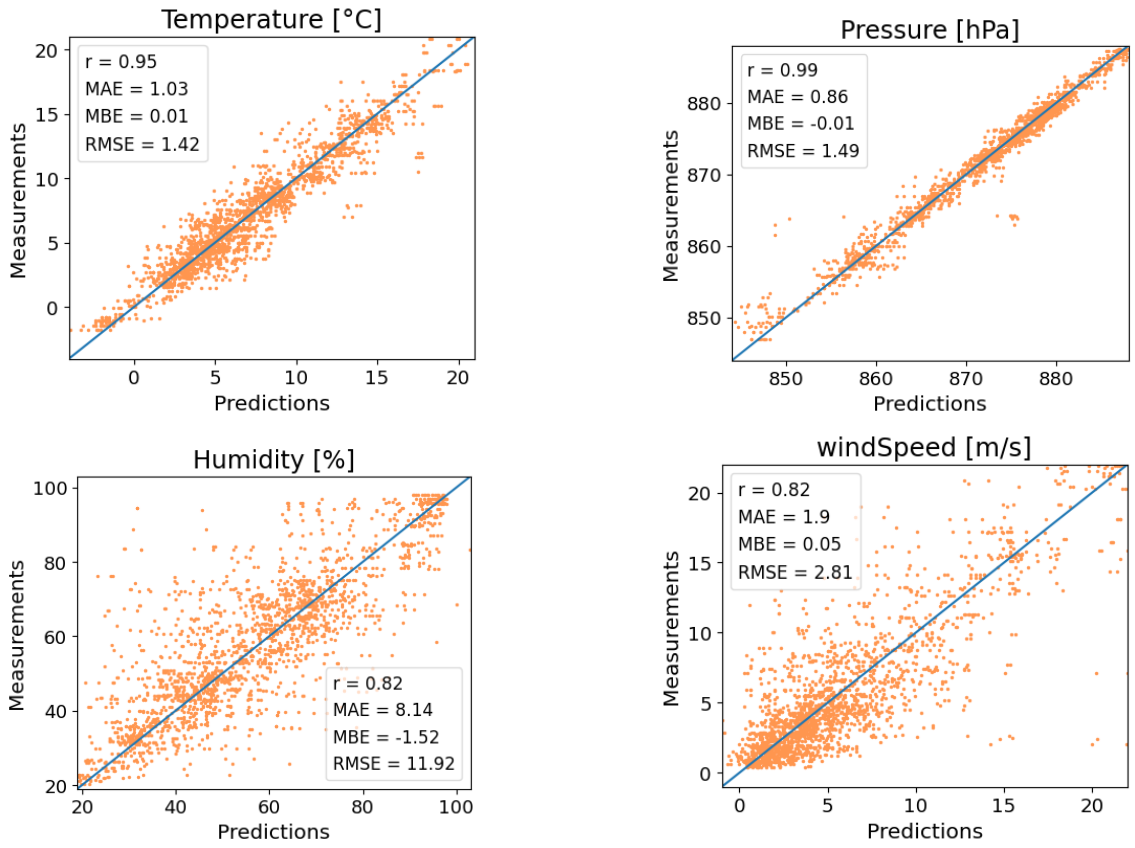

Figure 9: Comparison for 500 predictions of 4 hours each with the measurements data from CATS for the weather parameters.

Figure 9 present the correlation between the predictions and the measurements. For atmospheric pressure, it stands out as the parameter with the most accurate predictions, primarily due to its dependence on altitude, which remains relatively constant. The predicted values from the SARIMA model closely align with those recorded by the CATS weather station. The correlation coefficient exceeds 95%. Temperature is also well-predicted, displaying a correlation coefficient of over 90%. The correlation coefficient for wind speed reaches 80%. Wind speed is highly sensitive to topography and surface effects, so its accuracy at ground level is usually hard to achieve. Relative humidity is a challenging parameter to measure accurately, yet it still exhibits a reasonable correlation, reaching more than 80%. Despite this, relative humidity has minimal impact on observations in the visible and near-infrared spectrum. Nevertheless, it holds significance as it can lead to condensation on telescope mirrors, making it an important factor to consider.

These results are encouraging, however, it would be beneficial to conduct a statistical analysis on a larger data set. Moreover, this model can be employed to forecast drone profile weather data, contributing to predictions of the OT parameters. This model holds significant potential for short-term weather forecasting.

6. CONCLUSION

In this study, the WRF model was used to predict vertical profiles of meteorological parameters and to estimate the OT parameters (vertical profile of C_n^2) over Calern Observatory site. To evaluate WRF model performances, results of the C_n^2 were compared with observational data coming from PML.
In order to compute the OT parameters, we used an empirical model deduced from a statistical analysis of radio soundings balloons. Vertical distributions of OT given by this model are in good agreement compared to PML. However, a gap persists in the ground layer. A Site Learning method was applied to improve the empirical model and has demonstrated a significant improvement of the C_n^2 prediction. Although the dispersion above the ground level still remains. To improve the predictions in the first 500 m above the ground we used a UAS DJI Matrice 600 Pro equipped with weather stations. We have injected the meteorological data collected using the UAS in the WRF model. The preliminary results of the weather parameters shows encouraging results. And achieving an improvement in weather parameter prediction will contribute to enhance the prediction of the OT parameters. Nevertheless, further statistical analysis is required.
In the near future, we intend to make a measurement campaign using the instrumented UAS to gather a substantial amount of data. This will allow us to derive a global conclusion on the prediction of the turbulence parameters. Also, we plan to extend the instrumented UAS capabilities by adding temperature sensors for a direct measurement of the structure constant of temperature fluctuations C_T^2. Additionally, the UAS data can then be used to better constrain the empirical optical turbulence model and improve its credibility for statistical studies that closely align with the actual conditions of the site.
On a related note, the preliminary results of the SARIMA model were in a good agreement with measurements. It is worthwhile to expand this study and apply this model to drone data, potentially yielding accurate predictions for the OT parameters. Additionally, it's worth noting that these encouraging findings encourage the exploration of more advanced machine learning algorithms, which can prove highly beneficial for short-term predictions.

ACKNOWLEDGMENTS

We would like to thank the Centre National d'Études Spatiales (CNES) and the Université de la Côte d'Azur (UCA) for funding this activity. We acknowledge the NCEP/NCAR for the availability of the WRF model and and for providing public access to the GFS data. We also extend our thanks to SRTM for giving access to the high-resolution topographic data. We are also grateful to the Mesocentre SIGAMM of the Observatoire de la Côte d'Azur for hosting our model and for their help throughout the installation process.

REFERENCES

[1] C. Giordano et al. "Contribution of statistical site learning to improve optical turbulence forecasting". In: 504.2 (2021), pp. 1927–1938. DOI: 10.1093/mnras/staa3709.

[2] C. Giordano et al. "Statistical learning as a new approach for optical turbulence forecasting". In: 11448 (2020), 114484E. DOI: 10.1117/12.2562316.

[3] A. Rafalimanana et al. "Towards an optimal prediction of the optical turbulence in the ground layer by means of an instrumented drone". In: Society of Photo-Optical Instrumentation Engineers (SPIE) Conference Series 12185 (2022). DOI: 10.1117/12.2630032.

[4] Alohotsy Rafalimanana et al. "Optimal Prediction of Atmospheric Turbulence by Means of the Weather Research and Forecasting Model". In: *Publications of the Astronomical Society of the Pacific* 134.1035 (May 2022), p. 055002. DOI: 10.1088/1538-3873/ac6536.

[5] Hervé Trinquet and Jean Vernin. "A statistical model to forecast the profile of the index structure constant C_N^2". In: *Environmental Fluid Mechanics* 7.5 (2007), pp. 397–407. DOI: 10.1007/s10652-007-9031-x.

[6] Ziad, A. et al. "First results of the PML monitor of atmospheric turbulence profile with high vertical resolution". In: *A&A* 559 (2013). DOI: 10.1051/0004-6361/201322468.